



Swine manure management by hydrothermal carbonization: Comparative study of batch and continuous operation

R.P. Ipiates^{a,b}, A. Sarrion^a, E. Diaz^a, M.A. de la Rubia^a, E. Diaz-Portuondo^b, Charles J. Coronella^c, A.F. Mohedano^{a,*}

^a Chemical Engineering Department, Universidad Autónoma de Madrid, 28049, Madrid, Spain

^b Arquimea-Agrotech, 28400, Collado Villalba, Madrid, Spain

^c Department of Chemical and Materials Engineering, University of Nevada, Reno, Reno, 89557, Nevada, United States

ARTICLE INFO

Keywords:

Continuous reactor
Hydrochar combustion
Hydrothermal carbonization
Swine manure

ABSTRACT

Hydrothermal carbonization (HTC) is considered a promising technology for biomass waste management without pre-drying. This study explores the potential for swine manure management by comparing batch and continuous processes, emphasizing the benefits of the continuous mode, particularly for its potential full-scale application. The continuous process at low temperature (180 °C) resulted in a hydrochar with a lower degree of carbonization compared to the batch process, but similar characteristics were found in both hydrochars at higher operating temperatures (230–250 °C), such as C content (~ 52 wt%), fixed carbon (~ 24 wt%) and higher calorific value (21 MJ kg⁻¹). Thermogravimetric and combustion analyses showed that hydrochars exhibited characteristics suitable as solid biofuels for industrial use. The process water showed a high content of organic matter as soluble chemical oxygen demand (7–22 g L⁻¹) and total organic carbon (4–10 g L⁻¹), although a high amount of refractory species such as N- and O-containing long aromatic compounds were detected in the process water from the batch process, while the process water from the continuous process presented more easily biodegradable compounds such as acids and alcohols, among others. The longer time required to reach operating temperature in the case of the batch system (longer heating time to reach operating temperature) resulted in lower H/C and O/C ratios compared to hydrochar from the continuous process. This indicates that the dehydration and decarboxylation reactions of the feedstock play a more important role in the batch process. This study shows the efficiency of the continuous process to obtain carbonaceous materials suitable for use as biofuel, providing a solution for swine manure management.

1. Introduction

Hydrothermal carbonization (HTC) is an emerging technology to transform a wide range of biomass waste with high moisture content (>40%) (Heidari et al., 2020), such as sewage sludge (Reißmann et al., 2020), animal manure (Marin-Batista et al., 2020a), lignocellulosic biomass (Ipiates et al., 2022), or food waste (Mannarino et al., 2022), into a valuable carbon-rich and stable material called hydrochar, and an aqueous fraction, so-called process water, rich in soluble organic matter and potentially macronutrients. In addition, HTC allows removing and/or reducing harmful pollutants, such as pathogens, minimizing nasty odor dispersion and avoiding the landfill disposal from biomass waste (Fang et al., 2018). The resulting solid exhibits improved physical and chemical properties in comparison to raw biomass waste, such as

higher carbon (C) and lower oxygen (O) and hydrogen (H) content due to dehydration and decarboxylation processes of the feedstock. Furthermore, the C present in hydrochar is enriched in aromatic compounds, highly stable over time, and possesses greater energy density (Inkhoua et al., 2023). Furthermore, HTC reactions increase the fixed carbon (FC) content and therefore the energy density, regulating the combustion stability as well as the performance during the combustion of carbonaceous solids. These significant physicochemical changes in hydrochar open up diverse potential applications in various fields, such as biofuel (Ipiates et al., 2023a), soil amendment (Suarez et al., 2023), carbon sequestration (Islam et al., 2021) or active carbon precursor (Ding et al., 2022), among others. On the other hand, process water is a source of soluble organic matter such as oligosaccharides, sugars, volatile fatty acids (VFA), furfural, lignin fragments as well as nutrients i.e.,

* Corresponding author.

E-mail address: angelf.mohedano@uam.es (A.F. Mohedano).

<https://doi.org/10.1016/j.envres.2023.118062>

Received 31 October 2023; Received in revised form 11 December 2023; Accepted 26 December 2023

Available online 27 December 2023

0013-9351/© 2023 The Authors. Published by Elsevier Inc. This is an open access article under the CC BY-NC license (<http://creativecommons.org/licenses/by-nc/4.0/>).

phosphorus, calcium, and potassium, among others. The liquid fraction holds inherent potential to valorize through anaerobic digestion (Ipiales et al., 2021), nutrients recovery (Sarrion et al., 2023), microalgae growth substrate, or liquid fertilizer (Heidari et al., 2019).

So far, studies conducted on HTC of biomass residues have been mainly in laboratory-scale batch reactors. Only a limited number of studies have been reported in the literature using continuous reactors (Hoekman et al., 2017; Lucian et al., 2021; Zaccariello et al., 2022). In addition, there are approaches that perform simulation studies (Aragón-Briceño et al., 2020; Medina-Martos et al., 2020) or carry out numerical comparisons of possible full-scale HTC implementation (Heidari et al., 2020; Saba et al., 2019). Moreover, techno-economic analysis (Medina-Martos et al., 2020; Saba et al., 2019), life cycle assessments (Benavente et al., 2017; Meisel et al., 2019), kinetic studies or considerations for the design of continuous HTC reactors (Ruiz et al., 2020) are available in the literature. On the other hand, it should be noted that several companies have developed semi-industrial HTC plants for biomass waste management such as Ingelia (2023), AVACO₂ (Biochem, 2023), Terra Nova Energy (2023), HTCycle (HTCycle, 2023), among others.

The use of continuous reactors could offer advantages over batch reactors, including reduced energy, capital and labor costs, and better process control (Zaccariello et al., 2022). The existing literature lacks comprehensive information regarding continuous processes, and there are limited in-depth discussions concerning the constraints associated with HTC. These constraints encompass the origin and heterogeneity of feedstock, the quality of hydrochar, the potential for process water valorization, the utilization of catalysts, and energy consumption. Addressing these limitations within the context of a circular economy is crucial to improve the efficiency and cost-effectiveness of HTC technology. Current research is actively working to overcome these challenges, with the potential to improve the sustainability of waste management, which can provide a source of renewable energy and valuable raw materials/products, while involving effluent treatment processes to obtain recycled water.

Swine manure (SM) is a plentiful and readily available farm waste that is commonly managed using traditional disposal methods, including agricultural application, lagoon storage, anaerobic digestion or direct incineration (Varma et al., 2021; Wei et al., 2022). Currently, the swine sector presents additional challenges, including ethical concerns about animal confinement conditions, significant environmental impacts from large manure production from intensive livestock farming, and public health risks due to the overuse of antibiotics that fosters the emergence of resistant bacteria (Varma et al., 2021; Zahedi et al., 2022). The EU pig herd in 2023 is about 134 million head, with swine manure generation ≈ 182 Mt (d.b.) and responsible for about ≈ 118 Mt of CO₂ equivalent), accounting for about 9% of total GHG emissions from the agricultural sector (EEA, 2020). In Europe, swine lagoons are commonly employed as a method for storing and stabilizing residues produced in intensive livestock farming EU Directive 91/676/CEE (European Parliament, 2000). However, these lagoons generate significant negative environmental impacts due to the large quantities of waste they accumulate (Patil et al., 2023). Swine manure is a heterogeneous, dark-colored material composed mainly of fecal matter, urine, feed residues, detergent, bleach, insecticides, among others, which varies depending on specific farm characteristics such as animal category, age, type of feed, farm structure, cleaning system, among others. However, all SM waste shares common characteristics, including water content exceeding 90%, low organic matter concentration and a buffering capacity to regulate pH over 7 (Patil et al., 2023; Antezana et al., 2016). The SM is the largest contributor to GHG emissions from swine industry, accounting for around 70% of the total emissions (Hollas et al., 2021; Varma et al., 2021).

HTC is a potential alternative for swine manure management (Ipiales et al., 2023b; Lang et al., 2019a). Some studies have been conducted on HTC from swine manure, revealing various behaviors and qualities of

the products obtained. The resulting hydrochar presents improved properties compared to the initial feedstock, such as higher C, FC content and HHV (Smith et al., 2020). In the liquid fraction, a considerable amount of C is present in the form of soluble compounds, as well as elevated levels of NH₄-N (0.8–2.7 g L⁻¹) and PO₄-P (50–350 mg L⁻¹), along with other nutrients (Ipiales et al., 2023a; Lang et al., 2019). However, such studies on swine manure HTC have been limited to laboratory-scale experiments using batch reactors. This has resulted in a notable knowledge gap when comparing the performance and efficiency of batch versus continuous processes. In addition, there is a need to evaluate the scale-up potential of this technology for practical application on swine farming.

This study focuses specifically on investigating the differences in the utilization and management of swine manure by HTC using batch and continuous reactors. The research comprehensively analyzes the characteristics of the hydrochar yielded, with special emphasis on the impact of the heating ramp of both processes. The potential utilization of the hydrochar generated in the continuous process, evaluating its suitability as a biofuel, and exploring the feasibility of recovering nutrients and methane production by anaerobic digestion from the process water. The analysis and diversity of organic compounds in the process water are also examined, evaluating how they evolve with changes in temperature and operating mode. In addition, the study explores the possible application of the continuous reactor for swine manure management and utilization on pig farming, including a mass balance analysis.

2. Materials and methods

2.1. Feedstock origin

The solid fraction of swine manure (referred to as SM), employed for the HTC assays was obtained after centrifugation and separated from the liquid fraction at the pig farming. The SM was stored in sealed containers at room temperature. Table 1 shows the main characteristics of SM on a dry basis.

2.2. HTC experimental procedure

2.2.1. HTC in batch mode

HTC runs in batch mode were carried out in an electrically heated ZipperClave® pressure vessel of 4 L. In each sequence, the SM was blended with tap water up to 5% in TS. The HTC experiments were carried out with this mixture at four temperatures (180 °C, 210 °C, 230 °C and 250 °C) with a heating rate of 3 °C min⁻¹ and 45 min reaction time. The reactor was then cooled using an internal coil through which tap water was circulated at a cooling rate of around 10 °C min⁻¹. The slurry (hydrochar and process water) was separated by centrifugation (Orto Alresa centrifuge) at 8000 rpm for 10 min and filtration by a vacuum pump through membrane filters (0.45 µm). Wet hydrochar was dried at 105 °C overnight, ground and sieved (<250 µm), while the process water was stored at 4 °C. Hydrochar and process water were labeled according to the carbonization temperature and a letter B of batch mode i.e., HC180-B, PW180-B, etc.

The impact of the heating ramp (at 100 °C, 120 °C, 140 °C, 160 °C and 180 °C) on the characteristics of the solid and liquid phases was analyzed. Once the reactor reached the target temperature, the reaction was stopped suddenly using an internal cooling and immersing the reactor in an ice bath, thus inducing a fast temperature reduction. The solid and liquid fractions were labeled as “S” (solid phase) and “L” (liquid phase), respectively, followed by the operating temperature, i.e., S100, S120, L100, L120, etc.

2.2.2. Continuous HTC pilot plant

HTC runs in continuous mode were performed in a pilot plant developed collaboratively by the Chemical Engineering Department of Universidad Autonoma de Madrid and Arquimea Agrotech Company

Table 1

Main characteristics of hydrochar obtained from continuous and batch HTC of swine manure.

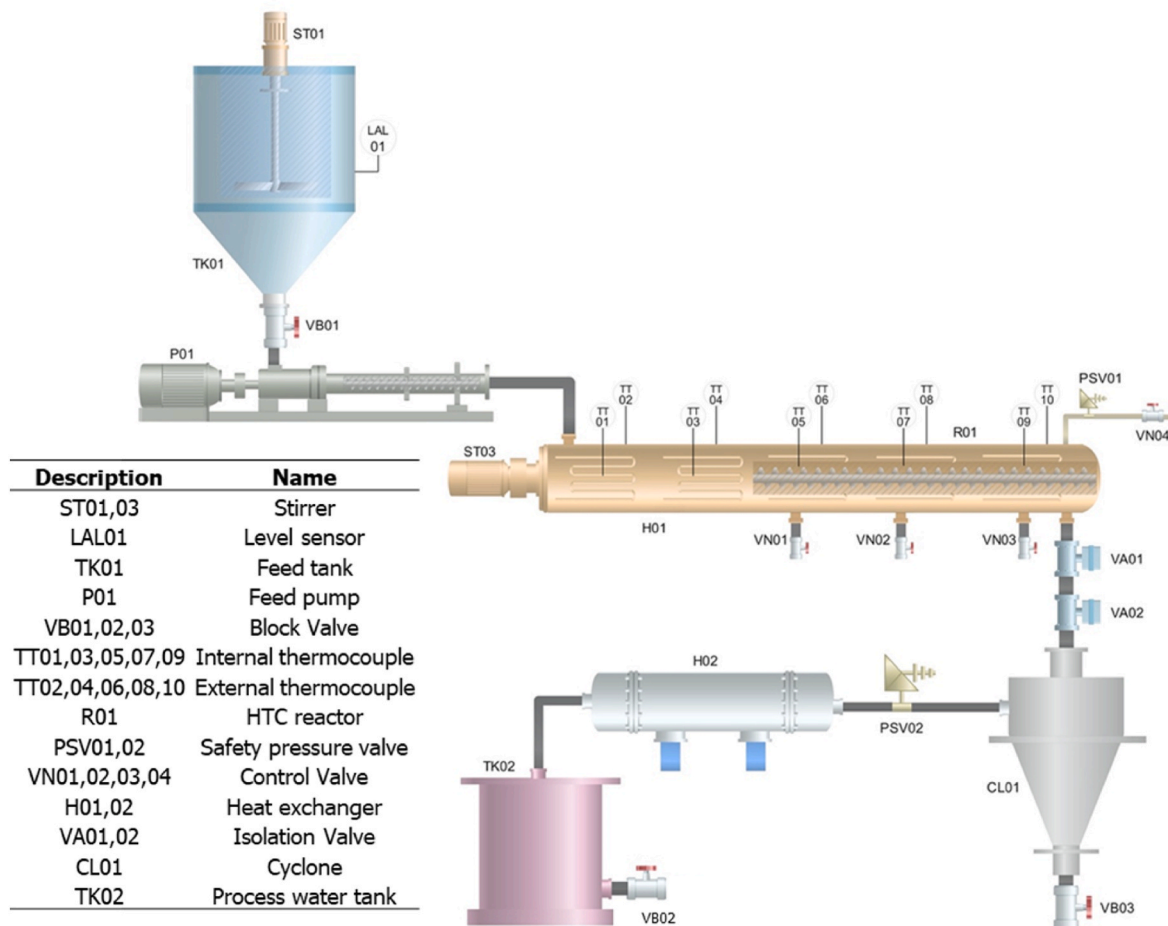
	SM	HC180-C	HC210-C	HC230-C	HC250-C	HC180-B	HC210-B	HC230-B	HC250-B
Y _{HC} (%)	–	71.8 (3.1) ^a	52.4 (2.4) ^b	46.2 (1.9) ^c	22.7 (0.6) ^d	42.9 (0.4) ^e	40.1 (0.5) ^e	35.2 (1.0) ^f	19.9 (0.6) ^g
FC (%)	13.7 (0.2) ^a	21.9 (0.3) ^b	21.2 (0.4) ^b	22.2 (0.3) ^b	23.5 (0.4) ^c	25.3 (0.4) ^d	24.2 (0.4) ^d	24.6 (0.2) ^d	25.0 (0.4) ^d
VM (%)	75.8 (0.1) ^a	74.6 (0.3) ^b	75.0 (0.4) ^b	73.8 (0.2) ^b	72.6 (0.2) ^c	71.2 (0.4) ^d	71.9 (0.3) ^d	70.6 (0.4) ^d	68.7 (0.1) ^e
Ash (%)	10.5 (0.1) ^a	3.5 (0.2) ^b	3.7 (0.1) ^b	3.9 (0.2) ^b	3.9 (0.2) ^b	3.5 (0.1) ^b	3.9 (0.2) ^b	4.8 (0.2) ^c	6.3 (0.2) ^d
C (%)	45.0 (0.4) ^a	47.1 (0.6) ^b	50.4 (0.3) ^c	51.5 (0.6) ^d	51.7 (0.5) ^d	50.0 (0.6) ^c	52.2 (0.6) ^d	53.0 (0.1) ^e	54.8 (0.3) ^e
N (%)	1.4 (0.0) ^a	0.8 (0.1) ^b	1.6 (0.3) ^a	1.4 (0.1) ^a	1.2 (0.1) ^a	1.4 (0.0) ^a	1.4 (0.1) ^a	1.5 (0.0) ^a	1.9 (0.0) ^c
S (%)	0.5 (0.0) ^a	0.3 (0.0) ^b	0.4 (0.0) ^b	0.2 (0.0) ^c	0.4 (0.0) ^b	0.3 (0.0) ^b	0.3 (0.0) ^b	0.3 (0.0) ^b	0.5 (0.0) ^a
H/C	1.52	1.45	1.35	1.32	1.34	1.38	1.25	1.19	1.07
O/C	0.62	0.65	0.57	0.54	0.54	0.64	0.58	0.50	0.47
HHV (MJ kg ⁻¹)	18.5 (0.2) ^a	18.8 (0.1) ^a	20.3 (0.3) ^b	20.7 (0.3) ^b	20.9 (0.2) ^c	19.9 (0.3) ^b	20.5 (0.4) ^b	21.0 (0.1) ^c	21.9 (0.2) ^d
E _{yield} (%)	–	73.2 (0.4) ^a	57.5 (0.2) ^b	51.7 (0.2) ^c	25.6 (0.4) ^d	46.2 (0.2) ^e	44.4 (0.3) ^e	40.0 (0.4) ^f	23.5 (0.1) ^d

Average values of three determinations with standard deviations.

a,b,c,d,e,f,g Means with different superscripts significant differ (p < 0.05).

(Arquimea, 2023). Fig. 1 shows a schematic diagram of continuous HTC unit. The pilot plant consists of a continuously stirred feeding tank that connects a screw pump to move the feedstock to the reactor. The reactor is a stainless-steel tube of 6 cm diameter, which includes an agitation system to prevent solids from settling and accumulating on the tube wall. The HTC reactor is divided into 5 zones: 2 for preheating and 3 for reaction. The exterior of the reactor is wrapped with electrical resistance heaters for temperature control. Slurry was depressurized through a sequence of two gate valves and was cooled with recirculating coolant provided by a chiller. The wet hydrochar was collected in a cyclone

vessel where the wet hydrochar is removed, while the process water goes into a storage tank. The HTC tests were conducted with the same swine manure and under the same operating conditions as the HTC batch runs (TS = 5%, T = 180 °C, 210 °C, 230 °C and 250 °C and 45 min residence time in the reaction zone). The wet hydrochar was filtered with a cloth filter with a pore diameter of 0.1 mm, and then dried at 105 °C. The process water was stored at 4 °C. Hydrochar and process water were labeled according to HTC temperature and a letter C of continuous mode i.e., HC180-C, PW180-C, HC210-C, etc. Each HTC run under batch or continuous mode was performed in triplicate.

**Fig. 1.** Schematic diagram of continuous HTC unit.

2.3. Analytical methods

2.3.1. Swine manure and hydrochar characterization

SM and hydrochars were characterized by proximate analysis (moisture, VM, FC and ash) performed using a Discovery SDT thermogravimetric analyzer (TG 209, F3, Netzsch; Selb, Germany) according to ASTM-D7582 (ASTM, 2015). Elemental composition (C, H, N, and S) was measured using a CHNS analyzer (LECO CHNS-932; Geleen, The Netherlands), while oxygen (O) was calculated by difference ($O = 100 - C - H - N - S - \text{ash}$ (wt%)). Mineral species and heavy metals were determined by inductively coupled plasma atomic emission spectroscopy (ICP-OES) after acid digestion on an Elan 6000 Sciex instrument (PerkinElmer; Santa Clara, United States). The morphology of hydrochars was assessed using scanning electron microscopy (SEM) and an energy dispersive X-ray analyzer within a Hitachi S-3000 N instrument (Hitachi Ltd, Tokyo, Japan). The images were obtained using a secondary electron (SE) and back-scattered electron (BSE) detector, in the high vacuum mode under an acceleration voltage of 20 kV.

Hydrochar mass yield (Y_{HC}) was calculated as the ratio of mass of hydrochar recovered (W_{HC}) to the mass of feedstock (W_{SM}), both on a dry basis (Eq. (1)).

$$Y_{HC}(\%) = \frac{W_{HC}}{W_{SM}} \cdot 100 \quad (1)$$

The HHV and energy yield (E_{yield}) of hydrochar were calculated using Eq. (2) (Schuster et al., 2001) and Eq. (3), respectively.

$$\begin{aligned} HHV (MJ \text{ kg}^{-1}) &= 0.3491 \cdot C + 1.033 \cdot H + 0.1005 \cdot S - 0.0151 \cdot N \\ &- 0.103 \cdot O - 0.0211 \cdot Ash \end{aligned} \quad (2)$$

$$E_{\text{yield}}(\%) = \frac{Y_{HC}(\%) \cdot HHV_{HC}}{HHV_{SM}} \quad (3)$$

The thermogravimetric (TG) analysis and derivative thermogravimetric (DTG) were conducted in a thermogravimetric analyzer (Discovery SDT 650), from 25 °C to 900 °C with an air flow rate of 100 mL min⁻¹ and a heating rate of 10 °C min⁻¹. Ignition temperature (T_i), burnout temperature (T_b), and peak temperature of the maximum loss weight (T_m) parameters of combustion and thermal behavior of fuels were measured by the DTG curve, while fuel ratio (FR) was calculated by Eq. (4).

$$FR = \frac{VM(\%)}{FC(\%)} \quad (4)$$

Slagging and fouling indexes were calculated based on the ash composition according to the equations described by (Tortosa et al., 2007) and modified by Cao et al. (2021). The analyses of feedstock and hydrochars were performed in triplicate.

2.3.2. Process water characterization

Process waters were characterized by pH (Crison 20 Basic pH-metre), TS, and volatile solids (VS) according to standard methods 2540 B and 2540 E, respectively (APHA, 2005). Soluble chemical oxygen demand (SCOD) was determined using APHA 5220D method (APHA, 2005). Total organic carbon (TOC) was determined by a Shimadzu TOC-VCPN analyzer (Shimadzu TOC Analyzers, Tokio- Japan). Soluble chemical oxygen demand (SCOD) were determined according method 5220D (APHA, 2005). The total Kjeldahl nitrogen (TKN) and ammonia nitrogen (NH_4-N) were determined by method 4500D and 4500 E, respectively (APHA, 2005). Organic nitrogen (Org-N) was determined by the difference between TKN and NH_4-N . The phosphorus content in the form of ortho phosphate (PO_4-P) was analyzed photometrically using a Hach Lange LCK350 cuvette test. Chemical species from process water were identified by gas chromatography/ion-trap mass spectrometry (GC-MS) on a CP-3800/Saturn 2200 instrument equipped with a Varian CP-8200 autosampler injector and a Carbowax/Divinyl benzene Yellow Green

solid-phase micro-extractor, and fitted with a Factor Four VF-5 MS capillary column (De la Rubia et al., 2018). The identification was established through a comparison with the NIST mass spectral library database. All the analysis and measurements were performed in triplicate.

2.4. Statistical analysis

The analytical results underwent rigorous statistical analysis using analysis of variance (ANOVA) within the GraphPad Prism 6.00 software. The minimum significant Fisher difference (Fisher LSD) was computed at a confidence level of 0.05. Multiple comparisons were performed to determine significant differences between the operating conditions of the HTC process.

3. Results and discussion

3.1. Hydrochar characteristics and potential uses

Table 1 lists the main characteristics of hydrochars obtained in the above-described batch and continuous reactors. The trends of Y_{HC} , C content, and HHV were similar in both processes. However, the Y_{HC} was much higher under continuous operation, especially at the lowest temperature 180 °C (72 wt%) compared with the batch process (~ 43 wt%), converging towards similar values at the highest temperature studied, 250 °C, differing by only 3 percentual points (p.p.), with a Y_{HC} to 23 wt % and 20 wt% from continuous and batch process, respectively. This suggests a convergence of performance between the two processes as the reaction temperature rises. This phenomenon may be attributed to the longer total residence time (preheating, reaction, and cooling) and the heating ramp to reach the reaction temperature in the batch HTC, which is noticeable at lower HTC temperatures. During batch HTC, the SM undergoes an extended preheating period spanning from 50 to 75 min in contrast to continuous HTC with shorter preheating time of 15 min. Within the preheating phase in both processes, the hydrolysis of less thermal stable components such as carbohydrates, lipids, and proteins is anticipated to occur, in soluble organic compounds into the process water (Singh et al., 2023). The compounds solubilized during the hydrolysis stage play a crucial role in the HTC process, acting as catalysts to increase the hydrolysis, dehydration, and decarboxylation of the initial biomass (Sharma et al., 2022), which, in terms of HTC, leads to enhance carbonization of the biomass. Furthermore, these soluble compounds also participate in aromatization and recondensation reactions, potentially forming secondary hydrochar (Gao et al., 2019). This has been more evident in HTC processes that recycle process water, where the soluble compounds obtained in the first cycle promote the decarboxylation of the new biomass, improving the C content, and HHV, reducing H/C and O/C atomic ratios, and significantly enhancing Y_{HC} (Antero et al., 2020). However, the HTC temperature increasing, seems to reduce the importance of preheating time and soluble organic compounds in Y_{HC} formation, due to uniform hydrolysis, decarboxylation, and dehydration at higher temperatures. This suggests the presence of a limit in temperature, residence time, and heating rate that represents an equilibrium point between hydrolysis and Y_{HC} production. In HTC with process water recirculation, Y_{HC} levels reach a steady state as the recycling cycle lengthens, despite the increasing concentration of organic species in the process water (Ding et al., 2022).

This phenomenon by heating ramp might account for the increased levels of FC, C, and HHV observed in the hydrochars produced through the batch process. Despite both processes were carried out at identical temperatures and reaction times, the statistical analysis reveals significant variations ($p > 0.05$) by the differences heating ramp. FC content in the hydrochars obtained in batch HTC was slightly higher (~ 25 wt%) than those obtained in the continuous process (21–23 wt%). Compared to the raw SM hydrochar from continuous HTC a negligible difference was observed in the VM content. The ash content decreased around 4–7

p. p., yielding the same effect on metal solubilization in both processes. The C content and H/C and O/C atomic ratios was lower in batch process. The C content in the hydrochar from batch process was in the range 50–55 wt% and hydrochar from continuous process in 47–52 wt%. The O/C and H/C atomic ratios exhibited comparable trends, reflecting a significant advancement in the dehydration and decarboxylation of the raw SM. The N and S content showed negligible variations ($p < 0.05$) in both processes and compared with initial SM. The HHV followed similar trends in both processes, gradually increasing with the increase in reaction temperature from 20 MJ kg⁻¹ to 19 MJ kg⁻¹ at 180 °C and 22 MJ kg⁻¹ and 21 MJ kg⁻¹ at 250 °C, reflecting an augmentation of 2–12% and 8–18% in the batch and continuous processes, respectively. However, the energy yield showed a decreasing trend with increasing temperature up to values $E_{\text{yield}} \sim 25\%$ on average at 250 °C in both processes, primarily linked to the low Y_{HC} .

3.1.1. Components distribution

Fig. 2 shows the distribution of C, N, and S in the hydrochar, process

water, and gas. In the batch process, the C retained in the hydrochar decreased from 51% to 27% (230–122 g C kg⁻¹ SM) from 180 °C to 250 °C, respectively, with a more pronounced decrease observed between 230 and 250 °C. In the continuous process, the decrease in the carbon content of hydrochar occurred gradually. At 180 °C, a value of 77% (347 g C kg⁻¹ SM) was reached, more than 25 p.p. higher than in the batch process. However, as the temperature increases, this disparity in C content decreases, reaching values of 31% (140 g C kg⁻¹ SM) at 250 °C close to that of the batch process (27%). The C content in the gas phase increases with carbonization temperature in the batch process from 4.5% to 10% (20–45 g C kg⁻¹ SM) from 180 °C to 250 °C, respectively. In the continuous process, the C content in the gas phase remains constant between 180 and 230 °C (7%, 32 g C kg⁻¹ SM), increasing to 10% at 250 °C, as in the batch process. This aligns with the O/C ratio, where higher temperatures correspond to increased decarboxylation. In the continuous process, the N content in the hydrochar followed a similar trend to the evolution of the C content, decreasing progressively with carbonization temperature, from 69% (9.2 g N kg⁻¹

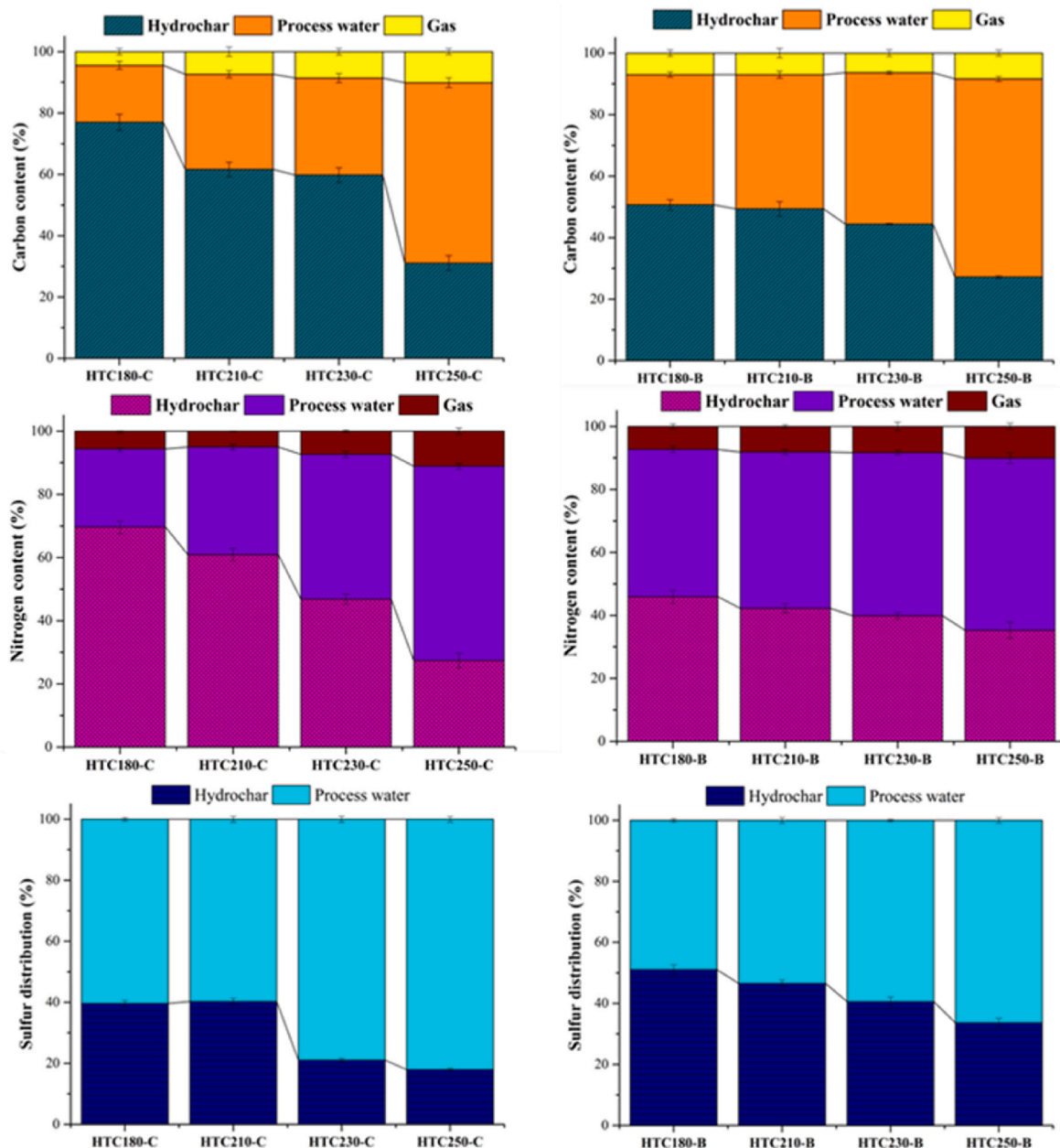


Fig. 2. Distribution of C, N and S of swine manure into hydrochar, process water and gas phase during the continuous and batch HTC.

SM) at 180 °C to 27% (3.6 g N kg⁻¹ SM) at 250 °C. In the batch process, the N content decreases steadily from 46% (6.1 g N kg⁻¹ SM) at 180 °C to 35% (4.7 g N kg⁻¹ SM) at 250 °C. The N content in the gas phase was reduced, reaching values of 7–10% in the batch process and 6–11% (0.8–1.6 g N kg⁻¹ SM) in the continuous process. Sulfur shows significant solubility in the process water, exceeding 50 wt% in all cases.

Fig. 3 depicts the distribution of the main elements present in the SM. The solubility of all elements increased with rising reaction temperature. This same trend is visible in both processes. The significant increase in solubility may be attributed to these elements initially are trapped within the biomass structure or in the form of organic molecules (such as phospholipids in the case of phosphorus). As the temperature rises, the extended hydrolysis of biomass can further enhance their solubility in the liquid phase. Ding et al. (2022), observed that at mild hydrothermal temperatures (<220 °C), the biomass structure largely maintains its integrity. However, at higher temperatures, the biomass structure experiences significant degradation. Table S1 displays the metal concentrations in the hydrochar. In the continuous process, metals generally exhibit a decrease in concentration in the hydrochar. However, in the case of P and Ca, they initially decrease but then increase to values similar to or even higher than the initial SM. Similar trends are observed in the batch process, with the exception of Ca and P, which showed significant increases even at mild temperatures 21–24 g C kg⁻¹ and 10–16 g P kg⁻¹, respectively. Despite the elements distribution (Fig. 3) showing a tendency to migrate away from the process water, the mass yield decreased dramatically with increasing temperature, dropping from 72 to 23 wt% in the continuous process and from 43 to 20 wt% in the batch process, respectively, compared with inorganic migration as seen in the ash content, only dropped by a few p.p. 5–7 p. p. Thus, although the temperature facilitated the migration of elements to the liquid fraction, the greater loss of mass resulted in an increase of metal concentration in the hydrochar. The heavy metal content (Table S1) also follows similar trends to the mineral metals. Despite the accumulation of certain metals (Ca and P) by weight, the predictive analysis of potential agglomeration and fouling of the hydrochars during oxidation (Table 2) indicates that both materials have medium fouling and corrosion risk (FI > 0.6, SI > 2.0 and AI > 0.34). Metals such as Ca, Mg, or Si are known to raise the ash fusion point, addressing related issues, thus despite the increase in these two metals, the ash agglomeration indexes are not significantly affected. In contrast, alkali metals such as Na and K can cause problems in combustion systems, leading to boiler fouling and reducing heat transfer efficiency (Mäkelä et al., 2016).

3.1.2. Thermogravimetric analysis

Fig. S1 depicts the TG and DTG profiles of hydrochars. The DTG curve exhibits two peaks corresponding to the oxidation of VM and thermally fewer stable compounds, followed by the oxidation of FC and thermally more stable compounds. Comparing hydrochars obtained at the same temperatures reveals no significant differences in the peak sizes. However, for HTC temperature >230 °C, it became evident that the peak corresponding to the VM gradually decreased, while the peak for FC showed a slight broadening due to a higher FC content (see Table 1). Some authors emphasize that a greater increase in the FC peak in the DTG profile indicates enhanced stability and release of useful energy in carbonaceous materials (Ma et al., 2021). This aligns with the context that high FC content, which is a more stable and energetically dense component, improves the combustion performance of carbonaceous solid combustion (Aliyu et al., 2021). The TG curve in all hydrochars shows a material loss of up to 90%, with the remainder corresponding to uncombusted ashes. The analysis of the combustion behavior (Table 2) reveals changes in their combustion characteristics mainly due to the VM and FC contents change. The T_i increased from 244 to 272 °C and from 272 to 284 °C in hydrochars obtained through continuous and batch HTC, respectively, with the discontinuous process having more relevance with a greater increase. The T_m did not show significant changes, remaining at an average temperature of 315 °C in all

cases. The most notable difference is observed in the T_b, which exhibits a gradual increase up to 530 °C, mainly due to the high FC content. This elevated T_i and T_b is reflected in the higher FR, which increased from 0.18 in SM to 0.32 and 0.36 in HC250–C and HC250–B, respectively. The analysis of combustion behavior indicates that the hydrochars exhibit greater thermal stability, potentially suggesting an improved combustion efficiency (Aliyu et al., 2021).

The features for hydrochar utilization as a biofuel are outlined in ISO/TS 17225–8 (2016) standard, which establishes parameters for the industrial-level usage of thermally treated biomass-derived solid biofuels. Both hydrochars derived from these processes exhibit suitable characteristics for industrial-level application as solid biofuels, owing to their higher energy densification (HHV >17 MJ kg⁻¹), low N (<3 wt%), S (<0.5 wt%), and ash (<10 wt%) contents, as well VM (<75 wt%). The SM presents high VM content (>75 wt%), thus cannot be directly employed as a biofuel due to the potential for rapid material consumption, shortcomings in thermal efficiency, and a reduced combustion performance. However, to achieve a high degree of carbonization and aromatization of hydrochar by HTC (H/C < 0.7 and O/C < 0.4 ratios) is not possible, as recommended by the European Biochar Certificate (EBC, 2019) for use in soil. This poses a challenge in preventing rapid degradation, soil erosion, or water retention issues in the potential uses of hydrochar as soil amendments. Solutions, such as post-treatments of hydrochar, have been proposed to address this challenge (Suarez et al., 2023). Furthermore, the elements analysis reveals that only Cu content exceeds the EU-established limit for heavy metals in fertilizer or soil amendments products (>100 mg kg⁻¹). The obtained hydrochar can be categorized to ornamental uses (European Union, 2019). The uses in agricultural soils (Agro- and Urban-category), the hydrochar requires post-treatment or blending with other materials (Suarez et al., 2023).

3.1.3. Heating ramp influence on hydrochar from batch HTC

Table 3 presents the characteristics of the solid material at different carbonization temperatures. During the carbonization process, certain organic components were hydrolyzed and transferred to the process water, resulting in a mass yield of 73 wt% at 100 °C, decreasing up to 50 wt% at 180 °C (S180). During the HTC process, the reduction in VM and FC increases, indicating the removal of less thermally stable compounds. The ash content, progressively decreases to values similar to those obtained at HC180 (~4 wt%) is observed. The C content initially increases to 46 wt% at 100 °C, then moderately decreases to 43 wt% at 120 °C. However, beyond 120 °C, C gradually rises, approaching the values obtained for HC180 values ~47 wt%. The N and S contents show minimal changes (p < 0.05) during the heating ramp, suggesting limited N and S migration to the liquid fraction. Despite this, there is a decrease in the atomic O/C and H/C ratios, indicating the influence of decarboxylation and dehydration reactions even at mild temperatures. Notably, the HHV of the solid at 120 °C–180 °C is lower than the initial material, mainly due to its reduced C content. However, HHV increases progressively as the temperature rises. Additionally, due to the loss of mass through hydrolysis reactions, the E_{yield} decreases to 48% with increasing temperature.

Fig. S2 displays the structural analysis of the SM, the profiles obtained during the heating ramp, and the hydrochars generated in both batch and continuous processes. At low carbonization temperature, the lignocellulosic components (lignin and cellulose) of the SM remained virtually unchanged, as shown in Fig. S2 (S100 and S160). However, as the temperature increased in both batch and continuous processes, the lignocellulosic structure underwent significant alteration, with almost complete disintegration observed at the highest tested temperature (250 °C). Furthermore, in the hydrochars, an aggregation of amorphous bodies can be observed, which may represent the accumulation of secondary hydrochar or other components such as precipitated salts within the main hydrochar structure (Taskin et al., 2019). These particles were not observed in S100 and S160, suggesting that at these temperatures,

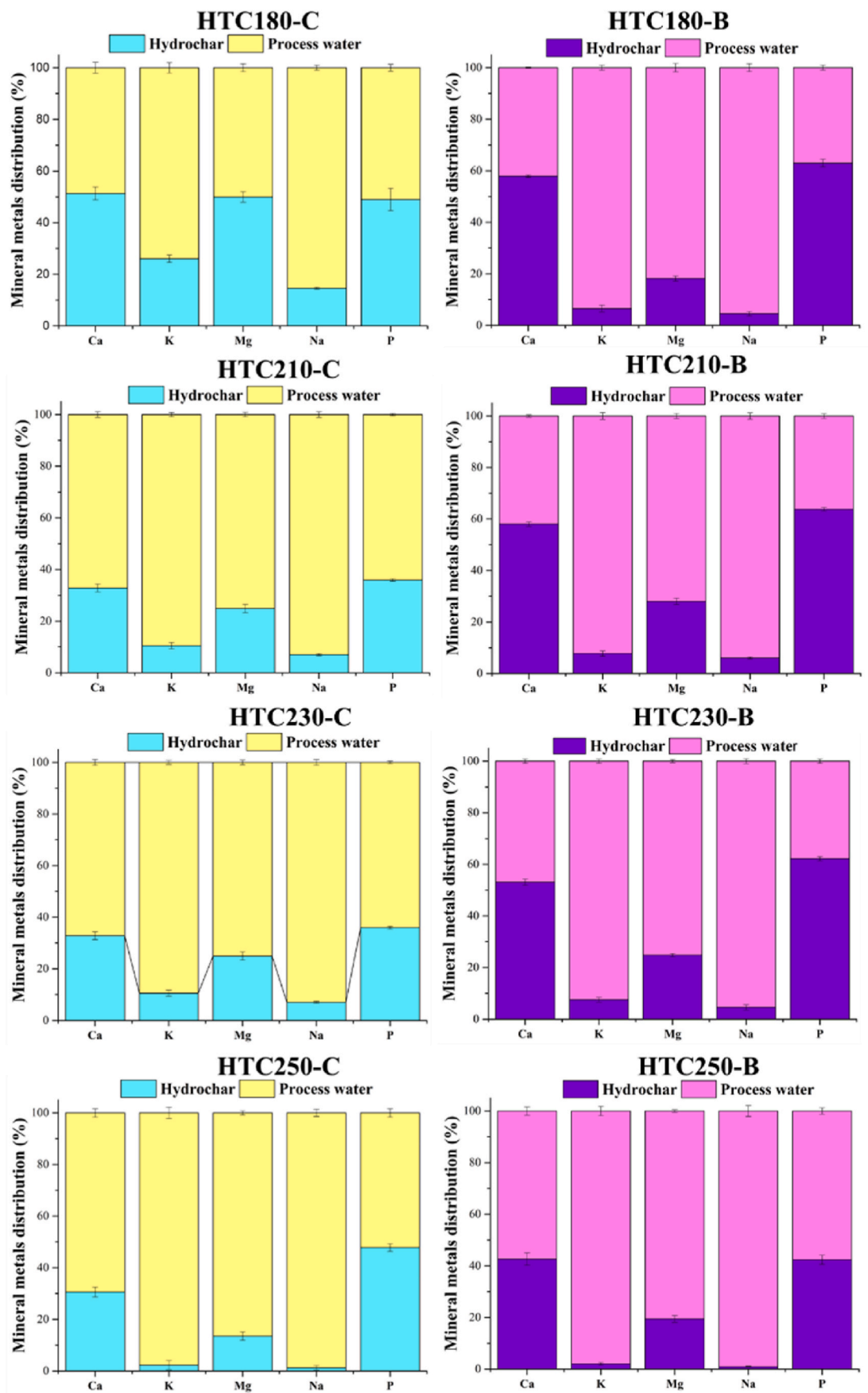


Fig. 3. Distribution of mineral species in products from batch and continuous HTC of swine manure.

Table 2

Ash agglomeration indexes and oxidation behavior of hydrochars from continuous and batch HTC of swine manure.

	Ash agglomeration propensity				Oxidation behavior			
	R _{b/a}	SI	FI	AI	T _i	T _m	T _b	FR
HC180-C	24.3	7.3	6.4	0.5	244	321	486	0.29
HC210-C	16.0	6.4	3.7	0.6	244	319	460	0.28
HC230-C	15.3	6.1	4.2	0.7	240	314	472	0.30
HC250-C	23.1	9.2	6.1	0.8	272	310	494	0.32
HC180-B	25.9	7.8	5.7	0.6	272	318	516	0.36
HC210-B	23.3	7.0	7.3	0.7	272	318	516	0.34
HC230-B	24.9	7.5	8.5	0.8	279	311	516	0.35
HC250-B	21.8	10.9	6.9	0.7	284	316	530	0.36

Table 3

Main characteristics of solid phase during the heating ramp in batch HTC of swine manure.

	S100	S120	S140	S160	S180
Y _{HC} (%)	73.0 (1.2) ^a	67.2 (1.0) ^b	63.4 (2.4) ^b	60.4 (0.6) ^c	49.6 (0.8) ^d
FC (%)	11.6 (0.2) ^a	16.3 (0.3) ^b	22.3 (0.1) ^c	22.5 (0.3) ^c	21.9 (0.2) ^c
VM (%)	81.7 (0.2) ^a	75.3 (0.4) ^b	67.1 (0.3) ^c	70.3 (0.3) ^d	74.2 (0.4) ^b
Ash (%)	6.7 (0.1) ^a	8.3 (0.2) ^b	10.6 (0.2) ^c	7.2 (0.3) ^d	3.8 (0.2) ^e
C (%)	46.2 (0.1) ^a	42.9 (0.1) ^b	45.3 (0.9) ^a	45.6 (2.5) ^a	46.4 (2.4) ^a
S (%)	0.5 (0.0) ^a	0.5 (0.0) ^a	0.4 (0.1) ^a	0.4 (0.1) ^a	0.4 (0.0) ^a
N (%)	1.4 (0.0) ^a	1.5 (0.1) ^a	1.3 (0.0) ^b	1.6 (0.0) ^a	1.3 (0.1) ^b
H/C	1.42	1.44	1.44	1.43	1.36
O/C	0.66	0.78	0.69	0.75	0.67
HHV (MJ kg ⁻¹)	18.3 (0.2) ^a	16.4 (0.1) ^b	17.9 (0.5) ^a	17.8 (1.4) ^a	18.0 (1.4) ^a
Eyield (%)	72.2 (0.7) ^a	59.6 (0.6) ^b	61.3 (1.1) ^c	58.1 (1.0) ^b	48.3 (1.0) ^d

Average values of three determinations with standard deviations.

a,b,c,d,e Means with different superscript significant differ ($p < 0.05$).

secondary hydrochar formation or ash agglomeration has not yet occurred. Additionally, the EDX analysis provides mineral distribution maps for all solids. In SM, S100 and S160, large solid particles are present (Fig. S3), which upon individual analysis, the identified particles could belong to calcium phosphates due to their high calcium and phosphorus spectra, likely originating from the swine's diet, including animal feed or supplements. Additionally, there are significant silicon-rich particles, likely coming from soil or sand in nearby farms. Sulfur-rich particles are also present, which could be linked to hair waste, proteins like cysteine and methionine, or common dietary supplements in animal feed (Trabue et al., 2022). After the hydrothermal process, these particles were degraded and significantly reduced in size, which is in agreement with the abovementioned increase migration of

inorganic elements from the hydrochar to the process water due to temperature rise (Fig. 3).

3.2. Process water characteristics

Table 4 shows the characteristics of both process waters. Batch HTC achieved a significantly higher Y_{PW} , averaging about twice as high (45–61%) as the continuous process (20–31%). This is supported by the high presence of organic matter in form of SCOD (16–21 g L⁻¹) and TOC (8–11 g L⁻¹) in batch process water. The organic matter in the batch process water surpasses that of the continuous reactor (SCOD 7–13 g L⁻¹ and TOC 4–11 g L⁻¹), although the difference decreases at the higher temperature analyzed. The process water obtained through continuous HTC exhibits a significant PO₄-P concentration (43–100 mg L⁻¹) against to 38–64 mg PO₄-P L⁻¹ in the batch process water. The high PO₄-P content in continuous process water could be due to the avoided P-complexes salts formation by the less global residence time. Sarrion et al. (2022), reported that residence times >30 min resulted in a ~ 30% decrease in PO₄-P content in the process water. The opposite trend is observed in the TN content with a gradual increment from 173 mg L⁻¹ to 294 mg L⁻¹ and from 617 mg L⁻¹ to 800 mg L⁻¹ from 180 to 250 °C in the continuous and batch processes, respectively. The same trend is observed in the NH₄-N content, where the batch process was more efficient in mineralizing organic nitrogen (proteins and amino acids) into NH₄-N.

Fig. S4, Tables S2 and S3 display the organic composition profiles and organic diversity of PW180 and PW250 from batch and continuous process water, respectively. Batch process waters (PW180-B and PW250-B) exhibit similar organic diversity with a high content of aromatic components (phenols, furfural, benzene, etc.), N- and O-heteroatoms (pyrazines, pyrimidines), and cyclic compounds, along with a low presence of aliphatic compounds. Whereas PW180-C was dominated by aliphatic compounds, specially acids, esters, and alcohols. However, at increasing the temperature (PW250-C), similar organic compounds diversity to the batch process waters were observed being rich in aromatic compounds and heteroatoms. This demonstrates that at higher temperatures, the hydrolyzed compounds continue to react through dehydration, decarboxylation, aromatization, and Maillard reactions, making them more complex and increasing their presence in the process water. The organic compounds complexity in the process water obtained at higher temperatures has been extensively studied in the literature (Gaur et al., 2020; Ipiates et al., 2022), indicating that these compounds are difficult to degrade either aerobically or anaerobically.

Table 5 displays the characteristics of the liquid fraction obtained during the heating ramp in batch HTC. At low temperatures, low Y_{PW} and solubilized organic matter are observed in the liquid fraction. Above 160 °C there is a notable increase in organic matter presence into the process water, with TS > 5 g L⁻¹, VS > 4 g L⁻¹, SCOD > 8 g L⁻¹, and TOC > 2 g L⁻¹ doubling the values of L140. This pattern is also observed in TN and N-NH₄, indicating the hydrolysis and mineralization of nitrogen

Table 4

Main characteristics of process water from continuous and batch HTC of swine manure.

	PW180-C	PW210-C	PW230-C	PW250-C	PW180-B	PW210-B	PW230-B	PW250-B
Y _{PW} (%)	20.0 (1.8) ^a	26.8 (0.5) ^b	30.3 (0.6) ^a	31.2 (0.5) ^c	44.5 (0.3) ^d	48.1 (0.4) ^c	47.7 (0.5) ^b	60.8 (0.7) ^f
TS (g L ⁻¹)	5.7 (0.5) ^a	6.8 (0.7) ^a	5.7 (0.3) ^a	8.2 (0.4) ^b	7.0 (0.8) ^{a,b}	9.0 (0.6) ^a	10.5 (0.5) ^a	11.4 (0.5) ^a
VS (g L ⁻¹)	5.3 (0.5) ^a	6.0 (0.9) ^b	4.8 (0.2) ^c	6.8 (0.4) ^b	5.6 (0.5) ^d	7.5 (0.3) ^c	8.9 (0.2) ^c	8.6 (0.4) ^a
SCOD (g L ⁻¹)	6.5 (0.2) ^a	10.2 (0.6) ^b	11.0 (0.5) ^b	12.6 (0.7) ^c	16.3 (0.2) ^d	18.8 (0.5) ^e	19.2 (0.5) ^f	20.9 (0.4) ^e
TOC (g L ⁻¹)	3.5 (0.1) ^a	6.1 (0.1) ^b	7.2 (0.2) ^c	11.0 (0.3) ^d	8.1 (0.2) ^e	9.5 (0.4) ^f	10.9 (0.1) ^f	10.7 (0.2) ^f
PO ₄ -P (mg L ⁻¹)	60.0 (0.6) ^a	68.8 (0.2) ^b	43.0 (0.1) ^c	99.5 (0.2) ^d	64.3 (0.3) ^b	38.0 (0.1) ^e	40.8 (0.2) ^c	52.3 (0.2) ^f
TN (mg L ⁻¹)	173.0 (1.2) ^a	267.0 (2.2) ^b	238.8 (2.5) ^b	294.0 (2.5) ^c	617.0 (1.4) ^d	641.0 (1.0) ^e	675.2 (1.4) ^f	800.0 (1.5) ^g
NH ₄ -N (mg L ⁻¹)	98.0 (2.2) ^a	98.0 (1.7) ^a	168.0 (1.2) ^b	185.6 (1.8) ^c	392.0 (1.0) ^d	366.0 (2.5) ^e	352.1 (1.6) ^e	495.3 (1.5) ^f
pH	6.0 (0.2) ^a	4.4 (0.4) ^b	4.0 (0.1) ^b	4.2 (0.1) ^b	4.3 (0.4) ^b	4.2 (0.1) ^b	3.8 (0.2) ^b	5.1 (0.2) ^c
Conductivity (mS cm ⁻¹)	0.9 (0.0) ^a	1.7 (0.1) ^b	1.5 (0.1) ^c	1.3 (0.1) ^d	1.8 (0.0) ^e	2.0 (0.1) ^f	2.0 (0.2) ^f	2.1 (0.1) ^f

Average values of three determinations with standard deviations.

a,b,c,d,e,f,g Means with different superscript significant differ ($p < 0.05$).

Table 5

Main characteristics of the liquid fraction during the heating ramp in batch HTC of swine manure.

	L100	L120	L140	L160	L180
Y _{FW} (%)	4.0 (1.0) ^a	4.2 (0.5) ^a	4.7 (0.5) ^a	10.4 (1.2) ^b	20.7 (1.0) ^c
TS (g L ⁻¹)	1.8 (0.1) ^a	1.9 (0.1) ^a	2.1 (0.0) ^a	4.7 (0.2) ^b	9.3 (0.0) ^b
VS (g L ⁻¹)	1.7 (0.2) ^a	1.5 (0.2) ^a	1.8 (0.2) ^a	4.2 (0.5) ^b	8.0 (0.1) ^c
COD (g L ⁻¹)	1.2 (0.1) ^a	2.6 (0.0) ^b	3.5 (0.2) ^c	8.2 (0.2) ^d	14.9 (0.3) ^e
TOC (g L ⁻¹)	0.4 (0.0) ^a	0.5 (0.1) ^a	0.8 (0.1) ^b	1.8 (0.0) ^c	4.6 (0.2) ^d
PO ₄ -P (mg L ⁻¹)	4.4 (0.2) ^a	3.7 (0.3) ^b	10.4 (0.2) ^c	29.8 (1.2) ^d	43.7 (1.0) ^e
TN (mg L ⁻¹)	132.0 (4.2) ^a	127.5 (3.0) ^a	123.1 (1.4) ^a	274.0 (3.1) ^b	297.1 (1.0) ^c
NH ₄ -N (mg L ⁻¹)	19.4 (0.4) ^a	17.5 (1.3) ^a	35.6 (1.0) ^b	90.3 (0.4) ^c	93.2 (0.7) ^c
pH	6.0 (0.2) ^a	5.8 (0.1) ^a	6.3 (0.1) ^a	5.9 (0.1) ^a	5.9 (0.1) ^a
Conductivity (mS cm ⁻¹)	1.2 (0.0) ^a	1.3 (0.0) ^b	1.1 (0.0) ^a	2.1 (0.1) ^c	2.5 (0.0) ^d

Average values of three determinations with standard deviations.

a,b,c,d,e Means with different superscript significant differ ($p < 0.05$).

compounds. Conductivity significantly increases at 160 °C, suggesting enhanced hydrolysis and greater migration of organic and inorganic compounds into the process water. The pH of the liquid fraction remains relatively stable, probably due to the low presence of acid organic compounds.

3.3. Assessing the feasibility of continuous HTC in a swine farm setting

Fig. S5 illustrates the scheme of traditional SM management on a usual pig farming and the potential implementation of the continuous HTC system for SM valorization. This includes complementary operations to process water valorization by phosphorus recovery and organic matter treatment through anaerobic digestion. Traditionally, in pig farming, SM is stored in a pond as mandated by Council Directive 91/676/EEC concerning the protection of waters against pollution caused by nitrates from agricultural sources (European Parliament, 2000), to stabilization (1–4 months) (Elwan et al., 2015). Subsequently, the manure is separated through centrifugation, where the solid fraction is composted to yield a byproduct that can be used as organic fertilizer for nearby agricultural soils. The liquid fraction undergoes coagulation-flocculation processes to remove suspended organic matter, resulting in sludge sent to landfill or incineration. The effluent is treated in biological reactors to remove ammoniacal nitrogen, producing a liquid fraction sent to wastewater treatment plants. The primary output of this system is organic fertilizer, considered a low-value product (Liu and Wang, 2019). Depending on compost characteristics, it can have a market value ranging from 50 to 100 € ton⁻¹. However, the process involves expenses such as managing and transporting sludge generated during coagulation-flocculation, with aerobic treatment costs of around 5–30 € ton⁻¹ (Varma et al., 2021). In contrast, treating SM lagoons costs 20 € m⁻³, and thermal drying and incineration of the solid fraction are estimated to cost 70 € ton⁻¹ and 15–30 € ton⁻¹, respectively (Shukla et al., 2023). Overall, for farms primarily focused on livestock, waste management or valorization remains a significant challenge. The new policies and the sustainable pursuit of primary resources Directive 2008/98/EC on waste and repealing certain Directives (European Parliament, 2020), or Directive 2018/2001/EC on the promotion of the use of energy from renewable sources (European Parliament, 2018), there is a drive to transform farms into self-sustaining bio-factories by fully utilizing their byproducts. The comprehensive proposal for valorization through HTC and complementary processes could represent an

opportunity for the management and valorization of animal excreta and other agricultural residues (Fig. S5).

Table 6 shows a mass balance of the potential products obtained in the HTC valorization of SM on a swine farm with an estimated generation of 20000 tons per year and TS 5%, along with a comparison with the traditional manure management process to produce organic fertilizer. The quantity of hydrochar is calculated based on the TS on SM and Y_{HC} (Table 1), while the potential for phosphorus rich salts (struvite) is determined by assessing the phosphorus migration to the liquid fraction at each studied temperature (see Fig. 3) and the struvite yield obtained by Sarrion et al. (2023). The methane production through anaerobic digestion is estimated using the biochemical methane potential (210 mL CH₄ g⁻¹ COD) determined by Ipiales et al. (2023a). In general, lower operating temperatures result in higher hydrochar (794 ton y⁻¹) and struvite (143 ton y⁻¹) yields due to the lower hydrolysis of SM and increased migration of P to the liquid fraction. The methane production potential through anaerobic digestion is approximately 46375 m³ STP y⁻¹ on average, with no significant variations. Preliminary techno-economic estimates in the literature suggest a price range of 80–120 € ton⁻¹ for hydrochar to achieve profitability in a potential HTC scale-up (López et al., 2021; Mannarino et al., 2022; Medina-Martos et al., 2020; Saba et al., 2019). The market price for carbonaceous materials is slightly higher, depending on their characteristics, ranging from 200 to 250 € ton⁻¹ (Hussin et al., 2023; Oliver-Tomas et al., 2019). Struvite prices can vary from 500 to 800 € ton⁻¹ (Mannarino et al., 2022; Nagarajan et al., 2023), while methane prices can be around 55 € MWh⁻¹ (EBA, 2022; European Commission, 2022).

Lucian et al. (2021) conducted an analysis of filtrability and nutrient utilization in the HTC of wastewater sludge using a continuous reactor at 200 °C and 15 bar of pressure. The results reveal that the produced hydrochar is more hydrophobic than the initial sludge, making the material up to 70% easier to dry. Furthermore, the excellent opportunity to recycle nutrients from wastewater sludge for the formation of inorganic salts rich in phosphorus with minimal heavy metal content. In addition, Ruiz et al. (2020) and Stemann and Ziegler (2011) examined the utilization of lignocellulosic biomass in a continuous and semi-continuous HTC reactors, discovering that the use of a continuous reactor provides an advantage for transforming waste into a carbonaceous solid for potential use as a biofuel. Additionally, it demonstrates high energy efficiency, making it an energetically sustainable process. Similar findings were reported by Zaccariello et al. (2022) indicating that HTC is an energy-efficient process.

The proposed approach, which involves HTC products and process water valorization, seems to offer a more profitable and promising alternative compared to traditional waste management. However, a comprehensive cost analysis is required, focusing on energy balance, integration, and overall implementation costs, including amortization, CAPEX, and OPEX, to assess sustainability and profitability. González-Arias et al. (2023) emphasize the importance of optimizing energy integration for the profitability and efficiency of the HTC process. Additionally, López et al. (2021) suggest that optimizing Y_{HC} can greatly improve the economic viability of HTC, due to methane and struvite constitute only a small portion compared to the potential hydrochar production as pointed out by Ipiales et al. (2023a). Co-carbonization between SM with lignocellulosic biomass to enhance

Table 6

Potential HTC products generation in a swine farm.

	Hydrochar (Ton year ⁻¹)	Methane (m ³ year ⁻¹)	Struvite (Ton year ⁻¹)
Compost	1106	–	–
HTC180	794	45879	143
HTC210	580	46420	126
HTC230	763	45956	115
HTC250	251	47247	122

HTC's economic viability by doubling the Y_{HC} , increasing HHV by 20% and improving the combustion performance of the hydrochars (Ipiales et al., 2023a; Lang et al., 2018). Further research is necessary to explore energy integration scenarios and maximizing synergy between complementary processes for efficient waste valorization.

4. Conclusions

The study evaluates the possible management of swine manure by hydrothermal carbonization in a batch reactor and in a continuous reactor at pilot plant scale. The characteristics of hydrochars and their suitability as biofuel for both processes are analyzed, considering the ISO/TS standards for solid biofuels from organic wastes treated by thermochemical processes. At low temperature (180 °C) the continuous process generated hydrochar with a lower degree of carbonization (C ~ 47 wt%, FC ~ 22 wt%, HHV 19 MJ kg⁻¹, H/C 1.45, and O/C 0.65) compared to the batch process, but these differences converged to similar values with increasing temperature (250 °C; C ~ 52 wt%, FC ~ 24 wt%, HHV 21 MJ kg⁻¹, H/C 1.34, and O/C 0.54). This highlights the positive impact of the heating ramp on the discontinuous process at low temperature that allows increasing the energy density of hydrochar. Thermogravimetric analysis, compared to ISO standards, indicated that both processes produce hydrochars suitable for a potential use as bio-fuel. The process water characteristics also showed differences between the batch and continuous process at low temperature to decrease as the carbonization temperature increased. The implementation of a continuous HTC reactor in a swine farm could be an interesting alternative for the management of swine manure, generating a product with alternative use to compost.

CRedit authorship contribution statement

R.P. Ipiales: Formal analysis, Investigation, Writing - original draft. **A. Sarrion:** Formal analysis, Investigation, Writing - original draft. **E. Diaz:** Funding acquisition, Resources, Supervision, Writing - review & editing. **M.A. de la Rubia:** Conceptualization, Funding acquisition, Methodology, Project administration, Resources, Supervision, Writing - review & editing. **E. Diaz-Portuondo:** Conceptualization, Formal analysis, Funding acquisition, Resources, Supervision. **Charles J. Coroneilla:** Conceptualization, Formal analysis, Funding acquisition, Resources, Supervision. **A.F. Mohedano:** Conceptualization, Funding acquisition, Methodology, Project administration, Resources, Supervision, Writing - review & editing.

Declaration of competing interest

The authors declare that they have no known competing financial interests or personal relationships that could have appeared to influence the work reported in this paper.

Data availability

Data will be made available on request.

Acknowledgements

Authors greatly appreciate funding from Spanish MCIN/AEI/10.13039/501100011033 and European Union "NextGenerationEU/PRTR" (TED2021-130287B-I00, PDC 2021-120755-I00, and PID 2022-138632OB-I00) and Grupo Kerbest Company. R.P. Ipiales acknowledges the financial support from the Community of Madrid (IND2019/AMB-17092) and Arquimea Agrotech Company. The authors thank M. Colas, R. Roncero and R. Gomez for their valuable help.

Appendix A. Supplementary data

Supplementary data to this article can be found online at <https://doi.org/10.1016/j.envres.2023.118062>.

References

- Aliyu, M., Iwabuchi, K., Itoh, T., 2021. Upgrading the fuel properties of hydrochar by co-hydrothermal carbonisation of dairy manure and Japanese larch (*Larix kaempferi*): product characterisation, thermal behaviour, kinetics and thermodynamic properties. *Biomass Convers. Biorefinery*. <https://doi.org/10.1007/s13399-021-02045-0>.
- Antero, R.V.P., Alves, A.C.F., de Oliveira, S.B., Ojala, S.A., Brum, S.S., 2020. Challenges and alternatives for the adequacy of hydrothermal carbonization of lignocellulosic biomass in cleaner production systems: a review. *J. Clean. Prod.* 252, 119899 <https://doi.org/10.1016/j.jclepro.2019.119899>.
- Antezana, W., De Blas, C., García-Rebollar, P., Rodríguez, C., Beccaccia, A., Ferrer, P., Cerisuelo, A., Moset, V., Estellés, F., Cambra-López, M., Calvet, S., 2016. Composition, potential emissions and agricultural value of pig slurry from Spanish commercial farms. *Nutrient Cycl. Agroecosyst.* 104, 159–173. <https://doi.org/10.1007/s10705-016-9764-3>.
- APHA, 2005. *Standard Methods for the Examination of Water and Wastewater, twenty-first ed.* American Public Health Association, Washington, DC., USA.
- Aragón-Briceño, C.I., Grasham, O., Ross, A.B., Dupont, V., Camargo-Valero, M.A., 2020. Hydrothermal carbonization of sewage digestate at wastewater treatment works: influence of solid loading on characteristics of hydrochar, process water and plant energetics. *Renew. Energy* 157, 959–973. <https://doi.org/10.1016/j.renene.2020.05.021>.
- Arquimea, 2023. Arquimea [WWW Document]. URL: <https://www.arquimea.com/es/>.
- ASTM, 2015. *Standard Test Methods for Proximate Analysis of Coal and Coke by Macro Thermogravimetric Analysis*. ASTM-International, Pennsylvania. <https://doi.org/10.1520/D7582-15>. Method D7582-15.
- Benavente, V., Fullana, A., Berge, N.D., 2017. Life cycle analysis of hydrothermal carbonization of olive mill waste: comparison with current management approaches. *J. Clean. Prod.* 142, 2637–2648. <https://doi.org/10.1016/j.jclepro.2016.11.013>.
- Biochem, A., 2023. No title [WWW Document]. URL: <https://ava-biochem.com/>.
- Cao, Z., Hülsemann, B., Wüst, D., Oechsner, H., Lautenbach, A., Kruse, A., 2021. Effect of residence time during hydrothermal carbonization of biogas digestate on the combustion characteristics of hydrochar and the biogas production of process water. *Bioresour. Technol.* 333, 125110 <https://doi.org/10.1016/j.biortech.2021.125110>.
- De la Rubia, M.A., Villamil, J.A., Rodríguez, J.J., Borja, R., Mohedano, A.F., 2018. Mesophilic anaerobic co-digestion of the organic fraction of municipal solid waste with the liquid fraction from hydrothermal carbonization of sewage sludge. *Waste Manag.* 76, 315–322. <https://doi.org/10.1016/j.wasman.2018.02.046>.
- Ding, Y., Guo, C., Qin, S., Wang, B., Zhao, P., Cui, X., 2022. Effects of process water recirculation on yields and quality of hydrochar from hydrothermal carbonization process of rice husk. *J. Anal. Appl. Pyrolysis* 166, 105618. <https://doi.org/10.1016/j.jaap.2022.105618>.
- EBA, 2022. *European Biogas Association Annual Report 28*.
- EBC, 2019. *Guidelines for a Sustainable Production of Biochar*. European Biochar Certificate. <https://doi.org/10.13140/RG.2.1.4658.7043>.
- EEA, 2020. *Bio-waste in Europe-Turning challenges into opportunities*. Copenhagen. <https://doi.org/10.2800/630938>.
- Elwan, A., Arief, Y.Z., Adzis, Z., Asiah, N., 2015. Life cycle assessment-based environmental impact comparative analysis of composting and electricity generation from solid waste. *Energy Proc.* 68, 186–194. <https://doi.org/10.1016/j.egypro.2015.03.247>.
- Energy, T., 2023. *Terranova energy* [WWW Document]. URL: <https://terranova-energy.com/en/>.
- European Commission, 2022. *Quarterly Report on European Gas Markets*. Brussel – Belgium.
- European Parliament, 2020. Directive 2008/122/EC of the European Parliament and of the Council, Fundamental Texts on European Private Law. <https://doi.org/10.5040/9781782258674.0028>.
- European Parliament, 2018. Directive (EU) 2018/2001 of the European Parliament and of the Council on the Promotion of the Use of Energy from Renewable Sources. *Official Journal of the European Union*.
- European Parliament, 2000. Protection of water against pollution caused by nitrates from agricultural sources. *Off. J. Eur. Communities L* 269, 1–15.
- European Union, 2019. Regulation, E. U. (2019). 1009 of the European Parliament and of the Council of 5 June 2019 Laying Down Rules on the Making Available on the Market of EU Fertilising Products and Amending Regulations (EC) No 1069/2009 and (EC) No 1107/2009 and Repealing R.
- Fang, J., Zhan, L., Sik, Y.O., Gao, B., 2018. Minireview of potential applications of hydrochar derived from hydrothermal carbonization of biomass. *J. Ind. Eng. Chem.* 57, 15–21. <https://doi.org/10.1016/j.jiec.2017.08.026>.
- Gao, L., Volpe, M., Lucian, M., Fiori, L., Goldfarb, J.L., 2019. Does hydrothermal carbonization as a biomass pretreatment reduce fuel segregation of coal-biomass blends during oxidation? *Energy Convers. Manag.* 181, 93–104. <https://doi.org/10.1016/j.enconman.2018.12.009>.
- Gaur, R.Z., Khoury, O., Zohar, M., Poverenov, E., Darzi, R., Laor, Y., Posmanik, R., 2020. Hydrothermal carbonization of sewage sludge coupled with anaerobic digestion: integrated approach for sludge management and energy recycling. *Energy Convers. Manag.* 224, 113353 <https://doi.org/10.1016/j.enconman.2020.113353>.

- González-Arias, J., Torres-Sempere, G., González-Castaño, M., Baena-Moreno, F.M., Reina, T.R., 2023. Hydrochar and synthetic natural gas co-production for a full circular economy implementation via hydrothermal carbonization and methanation: an economic approach. *J. Environ. Sci. (China)*. <https://doi.org/10.1016/j.jes.2023.04.019>.
- Heidari, M., Dutta, A., Acharya, B., Mahmud, S., 2019. A review of the current knowledge and challenges of hydrothermal carbonization for biomass conversion. *J. Energy Inst.* 92, 1779–1799. <https://doi.org/10.1016/j.joei.2018.12.003>.
- Heidari, M., Salaudeen, S., Norouzi, O., Acharya, B., Dutta, A., 2020. Numerical comparison of a combined hydrothermal carbonization and anaerobic digestion system with direct combustion of biomass for power production. *Processes* 8 (43), 1–13. <https://doi.org/10.3390/pr8010043>.
- Hoekman, S.K., Broch, A., Felix, L., Farthing, W., 2017. Hydrothermal carbonization (HTC) of loblolly pine using a continuous, reactive twin-screw extruder. *Energy Convers. Manag.* 134, 247–259. <https://doi.org/10.1016/j.enconman.2016.12.035>.
- Hollas, C.E., Bolsan, A.C., Chini, A., Venturin, B., Bonassa, G., Cândido, D., Antes, F.G., Steinmetz, R.L.R., Prado, N.V., Kunz, A., 2021. Effects of swine manure storage time on solid-liquid separation and biogas production: a life-cycle assessment approach. *Renew. Sustain. Energy Rev.* 150, 111472 <https://doi.org/10.1016/j.rser.2021.111472>.
- HTCycle, 2023. HTCcycle [WWW Document]. URL <https://htcycle.ag/>.
- Hussain, F., Hazani, N.N., Khalil, M., Aroua, M.K., 2023. Environmental life cycle assessment of biomass conversion using hydrothermal technology: a review. *Fuel Process. Technol.* 246, 107747 <https://doi.org/10.1016/j.fuproc.2023.107747>.
- Ingelia, 2023. Ingelia [WWW Document]. URL <https://ingelia.com/>.
- Inkous, S., Li, C., Shao, Y., Lin, H., Fan, M., Zhang, L., Zhang, S., Hu, X., 2023. Co-hydrothermal carbonization of fruit peel with sugars or furfural impacts structural evolution of hydrochar. *Ind. Crops Prod.* 193, 116221 <https://doi.org/10.1016/j.indcrop.2022.116221>.
- Ipiates, R.P., de la Rubia, M.A., Diaz, E., Mohedano, A.F., Rodriguez, J.J., 2021. Integration of hydrothermal carbonization and anaerobic digestion for energy recovery of biomass waste: an overview. *Energy Fuel* 35, 17032–17050. <https://doi.org/10.1021/acs.energyfuels.1c01681>.
- Ipiates, R.P., Mohedano, A.F., Diaz-Portuondo, E., Diaz, E., De la Rubia, M.A., 2023a. Co-hydrothermal carbonization of swine manure and lignocellulosic waste: a new strategy for the integral valorization of biomass wastes. *Waste Manag.* 169, 267–275. <https://doi.org/10.1016/j.wasman.2023.07.018>.
- Ipiates, R.P., Mohedano, A.F., Diaz, E., de la Rubia, M.A., 2022. Energy recovery from garden and park waste by hydrothermal carbonisation and anaerobic digestion. *Waste Manag.* 140, 100–109. <https://doi.org/10.1016/j.wasman.2022.01.003>.
- Ipiates, R.P., Sarrion, A., Diaz, E., Diaz-Portuondo, E., Mohedano, A.F., de la Rubia, A., 2023b. Strategies to improve swine manure hydrochar: HCl-assisted hydrothermal carbonization versus hydrochar washing. *Biomass Convers. Biorefinery* 1–12. <https://doi.org/10.1007/s13399-023-04027-w>.
- Islam, Md Azharul, Limon, M.S.H., Romić, M., Islam, Md Atikul, 2021. Hydrochar-based soil amendments for agriculture: a review of recent progress. *Arabian J. Geosci.* 14 (102), 1–16. <https://doi.org/10.1007/s12517-020-06358-8>.
- ISO/TS 17225-8, 2016. International Organization for Standardization for Solid Biofuels – Fuel Specifications and Classes. TS 17225-8, first ed. Graded thermally treated and densified biomass fuels, USA.
- Lang, Q., Chen, M., Guo, Y., Liu, Z., Gai, C., 2019. Effect of hydrothermal carbonization on heavy metals in swine manure: speciation, bioavailability and environmental risk. *J. Environ. Manag.* 234, 97–103. <https://doi.org/10.1016/j.jenvman.2018.12.073>.
- Lang, Q., Guo, Y., Zheng, Q., Liu, Z., Gai, C., 2018. Co-hydrothermal carbonization of lignocellulosic biomass and swine manure: hydrochar properties and heavy metal transformation behavior. *Bioresour. Technol.* 266, 242–248. <https://doi.org/10.1016/j.biortech.2018.06.084>.
- Liu, Z., Wang, X., 2019. Manure Treatment and Utilization in Production Systems, Animal Agriculture: Sustainability, Challenges and Innovations. Elsevier Inc. <https://doi.org/10.1016/B978-0-12-817052-6.00026-4>.
- López, R., González-Arias, J., Pereira, F.J., Fernández, C., Cara-Jiménez, J., 2021. A techno-economic study of HTC processes coupled with power facilities and oxy-combustion systems. *Energy* 219, 119651. <https://doi.org/10.1016/j.energy.2020.119651>.
- Lucian, M., Merzari, F., Gubert, M., Messineo, A., Volpe, M., 2021. Industrial-scale hydrothermal carbonization of agro-industrial digested sludge: filterability enhancement and phosphorus recovery. *Sustain. Times* 13. <https://doi.org/10.3390/su13169343>.
- Ma, M., Bai, Y., Wang, J., Lv, P., Song, X., Su, W., Yu, G., 2021. Study on the pyrolysis characteristics and kinetic mechanism of cow manure under different leaching solvents pretreatment. *J. Environ. Manag.* 290, 112580 <https://doi.org/10.1016/j.jenvman.2021.112580>.
- Mäkelä, M., Fullana, A., Yoshikawa, K., 2016. Ash behavior during hydrothermal treatment for solid fuel applications. Part 1: overview of different feedstock. *Energy Convers. Manag.* 121, 402–408. <https://doi.org/10.1016/j.enconman.2016.05.016>.
- Mannarino, G., Sarrion, A., Diaz, E., Gori, R., De la Rubia, M.A., Mohedano, A.F., 2022. Improved energy recovery from food waste through hydrothermal carbonization and anaerobic digestion. *Waste Manag.* 142, 9–18. <https://doi.org/10.1016/J.WASMAN.2022.02.003>.
- Marin-Batista, J.D., Villamil, J.A., Qaramaleki, S.V., Coronella, C.J., Mohedano, A.F., De la Rubia, M.A., 2020. Energy valorization of cow manure by hydrothermal carbonization and anaerobic digestion. *Renew. Energy* 160, 623–632. <https://doi.org/10.1016/j.renene.2020.07.003>.
- Medina-Martos, E., Istrate, I.R., Villamil, J.A., Gálvez-Martos, J.L., Dufour, J., Mohedano, Á.F., 2020. Techno-economic and life cycle assessment of an integrated hydrothermal carbonization system for sewage sludge. *J. Clean. Prod.* 277, 122930 <https://doi.org/10.1016/j.jclepro.2020.122930>.
- Meisel, K., Clemens, A., Fühner, C., Breullmann, M., Majer, S., Thrän, D., 2019. Comparative life cycle assessment of HTC concepts valorizing sewage sludge for energetic and agricultural use. *Energies* 12, 786–802. <https://doi.org/10.3390/en12050786>.
- Nagarajan, A., Goyette, B., Raghavan, V., Bhaskar, A., Rajagopal, R., 2023. Nutrient recovery via struvite production from livestock manure-digestate streams: towards closed loop bio-economy. *Process Saf. Environ. Protect.* 171, 273–288. <https://doi.org/10.1016/j.psep.2023.01.006>.
- Oliver-Tomas, B., Hitzl, M., Owsianiak, M., Renz, M., 2019. Evaluation of hydrothermal carbonization in urban mining for the recovery of phosphorus from the organic fraction of municipal solid waste. *Resour. Conserv. Recycl.* 147, 111–118. <https://doi.org/10.1016/j.resconrec.2019.04.023>.
- Patil, P., Sharara, M., Shah, S., Kulesza, S., Classen, J., 2023. Impacts of utilizing swine lagoon sludge as a composting ingredient. *J. Environ. Manag.* 327, 116840 <https://doi.org/10.1016/j.jenvman.2022.116840>.
- Reißmann, D., Thrän, D., Blöhs, D., Bezama, A., 2020. Hydrothermal carbonization for sludge disposal in Germany: a comparative assessment for industrial-scale scenarios in 2030. *J. Ind. Ecol.* 1 <https://doi.org/10.1111/jiec.13073>. –15.
- Ruiz, H.A., Conrad, M., Sun, S.N., Sanchez, A., Rocha, G.J.M., Romaní, A., Castro, E., Torres, A., Rodríguez-Jasso, R.M., Andrade, L.P., Smirnova, I., Sun, R.C., Meyer, A. S., 2020. Engineering aspects of hydrothermal pretreatment: from batch to continuous operation, scale-up and pilot reactor under biorefinery concept. *Bioresour. Technol.* 299, 122685 <https://doi.org/10.1016/j.biortech.2019.122685>.
- Saba, A., McGaughey, K., Toufiq Reza, M., 2019. Techno-economic assessment of co-hydrothermal carbonization of a coal-Miscanthus blend. *Energies* 12 (630), 1–17. <https://doi.org/10.3390/en12040630>.
- Sarrion, A., de la Rubia, A., Coronella, C., Mohedano, A.F., Diaz, E., 2022. Acid-mediated hydrothermal treatment of sewage sludge for nutrient recovery. *Sci. Total Environ.* 156494 <https://doi.org/10.1016/j.scitotenv.2022.156494>.
- Sarrion, A., Ipiates, R.P., de la Rubia, M.A., Mohedano, A.F., Diaz, E., 2023. Chicken meat and bone meal valorization by hydrothermal treatment and anaerobic digestion: biofuel production and nutrient recovery. *Renew. Energy* 204, 652–660. <https://doi.org/10.1016/j.renene.2023.01.005>.
- Schuster, G., Weigl, K., Hofbauer, H., 2001. Biomass steam gasification and extensive parametric modeling study. *Bioresour. Technol.* 77, 71–79. [https://doi.org/10.1016/S0960-8524\(00\)00115-2](https://doi.org/10.1016/S0960-8524(00)00115-2).
- Sharma, H.B., Panigrahi, S., Vanapalli, K.R., Cheela, V.R.S., Venna, S., Dubey, B., 2022. Study on the process wastewater reuse and valorisation during hydrothermal co-carbonization of food and yard waste. *Sci. Total Environ.* 806, 1–15. <https://doi.org/10.1016/j.scitotenv.2021.150748>.
- Shukla, A., Patwa, A., Parde, D., Vijay, R., 2023. A review on generation, characterization, containment, transport and treatment of fecal sludge and septage with resource recovery-oriented sanitation. *Environ. Res.* 216, 114389 <https://doi.org/10.1016/j.envres.2022.114389>.
- Singh, R., Kumar, R., Sarangi, P.K., Kovalev, A.A., Vivekanand, V., 2023. Effect of physical and thermal pretreatment of lignocellulosic biomass on biohydrogen production by thermochemical route: a critical review. *Bioresour. Technol.* 369, 128458 <https://doi.org/10.1016/j.biortech.2022.128458>.
- Smith, A.M., Ekpo, U., Ross, A.B., 2020. The influence of pH on the combustion properties of bio-coal following hydrothermal treatment of swine manure. *Energies* 13, 1–20. <https://doi.org/10.3390/en13020331>.
- Stemann, J., Ziegler, F., 2011. Assessment of the Energetic Efficiency of A Continuously Operating Plant for Hydrothermal Carbonisation of Biomass. *Environ. Sci. Eng.*, 56077452. <https://doi.org/10.3384/ECP11057125>.
- Suarez, E., Tobajas, M., Mohedano, A.F., Reguera, M., Esteban, E., de la Rubia, A., 2023. Effect of garden and park waste hydrochar and biochar in soil application: a comparative study. *Biomass Convers. Biorefinery* 0123456789. <https://doi.org/10.1007/s13399-023-04015-0>.
- Taskin, E., de Castro Bueno, C., Allegretta, I., Terzano, R., Rosa, A.H., Loffredo, E., 2019. Multianalytical characterization of biochar and hydrochar produced from waste biomasses for environmental and agricultural applications. *Chemosphere* 233, 422–430. <https://doi.org/10.1016/j.chemosphere.2019.05.204>.
- Tortosa Masia, A.A., Buhre, B.J.P., Gupta, R.P., Wall, T.F., 2007. Characterising ash of biomass and waste. *Fuel Process. Technol.* 88, 1071–1081. <https://doi.org/10.1016/j.fuproc.2007.06.011>.
- Trabue, S.L., Kerr, B.J., Scoggin, K.D., Andersen, D.S., van Weelden, M., 2022. Swine diets: impact of carbohydrate sources on manure characteristics and gas emissions. *Sci. Total Environ.* 825, 153911 <https://doi.org/10.1016/j.scitotenv.2022.153911>.
- Varma, V.S., Parajuli, R., Scott, E., Canter, T., Lim, T.T., Popp, J., Thoma, G., 2021. Dairy and swine manure management – challenges and perspectives for sustainable treatment technology. *Sci. Total Environ.* 778, 146319 <https://doi.org/10.1016/j.scitotenv.2021.146319>.
- Wei, Y., Liang, Z., Zhang, Y., 2022. Evolution of physicochemical properties and bacterial community in aerobic composting of swine manure based on a patent compost tray. *Bioresour. Technol.* 343, 126136 <https://doi.org/10.1016/j.biortech.2021.126136>.
- Zaccariello, L., Battaglia, D., Morrone, B., Mastellone, M.L., 2022. Hydrothermal carbonization: a pilot-scale reactor design for bio-waste and sludge pre-treatment. *Waste and Biomass Valorization* 13, 3865–3876. <https://doi.org/10.1007/s12649-022-01859-x>.
- Zahedi, S., Gros, M., Casabella, O., Petrovic, M., Luis, J., Pijuan, M., 2022. Occurrence of veterinary drugs and resistance genes during anaerobic digestion of poultry and cattle manures. *Sci. Total Environ.* 822, 153477 <https://doi.org/10.1016/j.scitotenv.2022.153477>.